PHYSICAL REVIEW D **87,** 114012 (2013)

NLO analytical solutions to the polarized parton distributions, based on the Laplace transformation

S. Atashbar Tehrani,[1,2,*] F. Taghavi-Shahri,[2,3,†] A. Mirjalili,[4,‡] and M. M. Yazdanpanah[5,§]

[1]*Department of Physics, Yazd Branch, Islamic Azad University, Yazd, Iran*
[2]*School of Particles and Accelerators, Institute for Research in Fundamental Sciences (IPM), P.O. Box 19395-5531, Tehran, Iran*
[3]*Department of Physics, Ferdowsi University of Mashhad, P.O. Box 1436, Mashhad, Iran*
[4]*Physics Department, Yazd University, 89195-741 Yazd, Iran*
[5]*Faculty of Physics, Shahid Bahonar University of Kerman, 76169-14111 Kerman, Iran*

(Received 5 December 2012; revised manuscript received 18 March 2013; published 13 June 2013)

By using the Laplace transformation, the analytical solutions of the Dokshitzer-Gribov-Lipatov-Altarelli-Parisi evolution equations at the leading-order and next-to-leading-order (NLO) approximations for the gluon, singlet, and nonsinglet quark polarization inside the nucleon are obtained. At NLO approximation, a second Laplace transformation is required. Complete NLO calculations need an iteration method, which we try to employ. As an efficiently mathematical tool, we employ the Jacobi polynomials to extract the polarized nucleon structure, using the analytical solutions for the polarized parton densities. Optimum nucleon structure functions are determined by a χ^2 analysis of the available experimental data, and their uncertainties are estimated by the Hessian method. Our results for nucleon and deuteron structure functions are in good agreement with all available experimental data and fitting parametrization models.

DOI: 10.1103/PhysRevD.87.114012 PACS numbers: 13.60.Hb, 12.39.−x, 14.65.Bt

I. INTRODUCTION

The nucleon spin crisis is still one of the most fundamental problems in hadron physics. Many experiments in deep inelastic scattering suggest that just a small fraction of the spin of the proton is carried by the intrinsic spin of its quark constituents. This discovery has challenged our understanding about the internal structure of the proton and inspired vast experimental and theoretical activity to understand the role of spin in the proton's internal structure. The key question is how the spin of the nucleon is distributed among its constituent partons. That is, the determination and understanding of the quarks and gluon spin distribution functions have became an important issue.

Block *et al.* in Refs. [1–6] showed that, by using the Laplace transformation, it is possible to solve the Dokshitzer-Gribov-Lipatov-Altarelli-Parisi (DGLAP) evolution equations directly and extracted parton distribution functions in the unpolarized case. The advantage of using such a technique is that it is clearer than other methods for solving the DGLAP equations and also involves numerically much more efficient outputs. In this method, the parton distribution functions at arbitrary Q^2 can be expressed as a convolution of these distributions at a starting Q_0^2 with an analytically defined kernel in terms of the ordinary variables. This technique makes this facility that the analytical solution for the polarized parton distribution functions (PPDFs) are obtained more strictly by using the related kernels. The outstanding analytical results have more transparency forms which control the calculations in a better way.

Following our recent work on analytical calculation of the polarized gluon distribution function by using the Laplace transformation [7], in the present paper we try to apply the new method, initialized by Block *et al.* [1–3] in the unpolarized case, to the polarized one to extract the PPDFs. Since a substantial part of the nucleon spin, about 40%, is carried by the polarized valence quarks, we focus here first on the valence quark polarization. In addition to its simplicity and also for transparency, study of the valence quark polarization is the simplest way to test the analytical solution of the DGLAP equations in the polarized case, based on the Laplace transformation technique. We then extend our calculations, considering the polarized singlet and gluon distributions. Therefore using the Laplace transform technique and finding the PPDFs and then the nucleon spin structure functions are the main aims in this paper.

This paper is organized as follows. In Sec. II, we follow the Block scenario for analytical solutions but in connection to the polarized DGLAP evolution equations of the nonsinglet, singlet, and gluon distributions in the leading-order (LO) approximation. In continuation, we apply this scenario to the next-to-leading-order (NLO) approximation. At this order of approximation, it is inevitable to use a second Laplace transform and employ an iteration process to obtain the polarized gluon and singlet distributions. In Sec. III, Jacobi polynomials and the PPDFs resulting from the Laplace transformation are used to extract the polarized nucleon structure functions. In Sec. IV, we discuss how to

*atashbar@ipm.ir
†f_taghavi@ipm.ir
‡a.mirjalili@yazd.ac.ir
§myazdan@mail.uk.ac.ir

parameterize the polarized nucleon structure function at an initial value of the energy scale. We then deal with the evolution of the nucleon structure functions. We introduce an analysis relating to a global χ^2 in Sec. V. How to minimize it is also discussed there. Description of the error calculations is done in Sec. VI. Section VII is devoted to the results and discussions. Finally, we give our conclusions in Sec. VIII.

II. ANALYTICAL SOLUTION TO THE POLARIZED DGLAP EQUATIONS

A. Leading-order case

According to Refs. [1–3], it is possible to solve analytically the coupled leading- and next-to-leading-order DGLAP evolution equations to extract the unpolarized parton distribution functions. This new method is based on the Laplace transformations. Here we employ this method in the polarized case and take into account the polarized parton distribution inside the nucleon. We will not give the details here and only review the method for extracting the polarized parton distribution functions.

The DGLAP evolution equations to extract the polarized nonsinglet (NS), singlet (S), and gluon densities can be written as follows [8–11]:

$$\frac{4\pi}{\alpha_s(Q^2)}\frac{\partial \delta F_{\rm NS}(x,Q^2)}{\partial \ln Q^2} = (\delta F_{\rm NS} \otimes (\delta P^0_{qq} + \cdots))(x,Q^2), \tag{1}$$

$$\frac{4\pi}{\alpha_s(Q^2)}\frac{\partial \delta F_S(x,Q^2)}{\partial \ln Q^2} = (\delta F_S \otimes (\delta P^0_{qq} + \cdots) + \delta G \otimes (\delta P^0_{qg} + \cdots))(x,Q^2), \tag{2}$$

$$\frac{4\pi}{\alpha_s(Q^2)}\frac{\partial \delta G(x,Q^2)}{\partial \ln Q^2} = (\delta F_S \otimes (\delta P^0_{gq} + \cdots) + \delta G \otimes (\delta P^0_{gg} + \cdots))(x,Q^2), \tag{3}$$

where δP^0_{ij} are the leading-order polarized splitting functions and the ellipses represent the higher-order expansion of the splitting functions. The $\otimes$ symbol in the above equations refers to the convolution integral in which the splitting functions in the right-hand side of Eqs. (1)–(3) are in fact functions of a variable such as $\frac{x}{z}$.

By using the new variable $\tau \equiv \frac{1}{4\pi}\int_{Q_0^2}^{Q^2} \alpha_s(Q'^2) d\ln Q'^2$, and also $x = e^{-\nu}$ and $z = e^{-w}$, then the DGLAP evolutions in Eqs. (1)–(3) can be written in terms of the τ, ν, and w variables as three coupled ordinary first-order differential equations. Following that by Laplace transformation, the convolution integrals in DGLAP evolutions can be converted from ν space to s space [6]. Therefore we arrive at the following equations:

$$\begin{aligned}
\frac{\partial \delta f_{\rm NS}}{\partial \tau}(s,\tau) &= \delta\Phi^{\rm LO}_{\rm NS}(s)\delta f_{\rm NS}(s,\tau),\\
\frac{\partial \delta f_S}{\partial \tau}(s,\tau) &= \delta\Phi^{\rm LO}_{S}(s)\delta f_S(s,\tau) + \delta\Theta^{\rm LO}_{S}(s)\delta g(s,\tau),\\
\frac{\partial \delta g}{\partial \tau}(s,\tau) &= \delta\Phi^{\rm LO}_{g}(s)\delta g(s,\tau) + \delta\Theta^{\rm LO}_{g}(s)\delta f_S(s,\tau).
\end{aligned} \tag{4}$$

As is obvious, $\delta\Phi$'s and δg's in Eq. (4) are related to the Laplace transform of splitting functions in the s space. The analytical expressions for the LO coefficients $\delta\Phi^{\rm LO}$ and $\delta\Theta^{\rm LO}$ can be found in Ref. [4].

1. Nonsinglet solution

We follow the method in Ref. [1] to obtain an analytical solution for the polarized parton distributions. Below, we describe briefly how to get the analytical solution for the distributions of the nonsinglet sector.

Using the new variables υ, w, and τ for the nonsinglet sector, $F_{\rm NS}(x,Q^2)$ in Eq. (1), which are related to the valence quark distributions, we achieve

$$\frac{\partial \delta \hat{F}_{\rm NS}}{\partial \tau} = \int_0^{\upsilon} \delta \hat{F}_{\rm NS}(w,\tau) e^{-(\upsilon - w)} \delta P^{\rm LO,ns}_{qq}(\upsilon - w) dw. \tag{5}$$

The Laplace transformation of Eq. (5) will give us a linear differential equation in terms of s and τ variables whose solution can be presented by [see Eq. (4)]

$$\delta f_{\rm NS}(s,\tau) \equiv e^{\tau\Phi^{\rm LO}_{\rm NS}}\delta f_{\rm NS}(s). \tag{6}$$

Now, by using the kernel $\delta K_{\rm NS}(\upsilon,\tau) \equiv \mathcal{L}^{-1}[e^{\tau\delta\Phi^{\rm LO}_{\rm NS}(s)};\upsilon]$, the nonsinglet sector $\delta F_{\rm NS}(x,Q^2)$ can be obtained via the convolution integral as in the following:

$$\delta \hat{F}_{\rm NS}(\upsilon,\tau) = \int_0^{\upsilon} \delta K_{\rm NS}(\upsilon - w,\tau)\delta \hat{F}_{\rm NS}(w) dw. \tag{7}$$

It is obvious that $\delta \hat{F}_{\rm NS}(w)$ in the right-hand side of Eq. (7) is related to this quantity at the initial energy scale. The final result in (x,Q^2) space can be obtained by using the appropriate change of variable, $\upsilon \equiv \ln(1/x)$.

2. Singlet and gluon solutions

With the initial conditions for singlet and gluon sectors of distributions, which are denoted by $\delta f^0_S(s)$ and $\delta g^0(s)$, respectively, their evolved solutions in the Laplace s space are given by [5]

$$\begin{aligned}
\delta f(s,\tau) &= \delta k_{ff}(s,\tau)\delta f^0_S(s) + \delta k_{fg_1}(s,\tau)\delta g^0(s),\\
\delta g(s,\tau) &= \delta k_{gg}(s,\tau)\delta g^0(s) + \delta k_{gf}(s,\tau)\delta f^0_S(s),
\end{aligned} \tag{8}$$

where the δk's in Eq. (8) have been introduced in Refs. [1,6].

The decoupled solutions of the polarized singlet and gluon distributions in (υ,τ) space can be written by the following convolution integrations:

$$\delta\hat{F}_S(\nu, Q^2) \equiv \int_0^\nu K_{FF}(\nu - w, \tau(Q^2, Q_0^2))\delta\hat{F}_S(w)dw + \int_0^\nu K_{FG}(\nu - w, \tau(Q^2, Q_0^2))\delta\hat{G}_S(w)dw,$$
$$\delta\hat{G}_S(\nu, Q^2) \equiv \int_0^\nu K_{GG}(\nu - w, \tau(Q^2, Q_0^2))\delta\hat{G}_S(w)dw + \int_0^\nu K_{GF}(\nu - w, \tau(Q^2, Q_0^2))\delta\hat{F}_S(w)dw, \quad (9)$$

where K's are the inverse Laplace transform of k's in Eq. (8). As in Eq. (7), $\delta\hat{F}_S$ and $\delta\hat{G}_S$ are related to singlet and gluon distributions, respectively, at the initial value of Q_0.

Recalling that $\nu \equiv \ln(1/x)$, we can finally back the above solutions into the usual Bjorken-x space.

B. Next-to-leading-order case

1. Nonsinglet solution

For the nonsinglet distribution $\delta F_{\rm NS}(x, Q^2)$, the logarithmic derivative of $\delta F_{\rm NS}$ can appear schematically as the convolution of $\delta F_{\rm NS}(x, Q^2)$ with the nonsinglet splitting functions $\delta P_{qq}^{\rm LO,NS}(x)$ and $\delta P_{qq}^{\rm NLO,NS}(x)$ for LO and NLO approximations, respectively, i.e.,

$$\frac{4\pi}{\alpha_s(Q^2)}\frac{\partial\delta F_{\rm NS}(x, Q^2)}{\partial\ln(Q^2)} = \delta F_{\rm NS} \otimes \left(\delta P_{qq}^{\rm LO,NS} + \frac{\alpha_s(\tau)}{4\pi}\delta P_{qq}^{\rm NLO,NS}\right)(x, Q^2). \quad (10)$$

After changing to the required variables which have been introduced in [1], we arrive at

$$\frac{\partial\delta\hat{F}_{\rm ns}}{\partial\tau}(\nu, \tau) = \int_0^\nu \delta\hat{F}_{\rm ns}(w, \tau)e^{-(\nu-w)}\left(\delta P_{qq}^{\rm LO,ns}(\nu - w) + \frac{\alpha_s(\tau)}{4\pi}\delta P_{qq}^{\rm NLO,ns}(\nu - w)\right)dw. \quad (11)$$

Going to Laplace space s, we obtain a linear differential equation with respect to the τ variable for the transformed $\delta f_{\rm NS}(s, \tau)$. Therefore we will arrive at

$$\frac{\partial\delta f_{\rm NS}}{\partial\tau}(s, \tau) = \left(\delta\Phi_{\rm NS}^{\rm LO}(s) + \frac{\alpha_s(\tau)}{4\pi}\delta\Phi_{\rm NS}^{\rm NLO}(s)\delta f(s, \tau)\right). \quad (12)$$

This has the simple solution

$$\delta f_{\rm NS}(s, \tau) = e^{\tau\delta\Phi_{\rm NS}(s)}\delta f_{\rm NS}^0(s), \quad (13)$$

where

$$\delta\Phi_{\rm NS}(s) \equiv \delta\Phi_{\rm NS}^{\rm LO}(s) + \frac{\tau_2}{\tau}\delta\Phi_{\rm NS}^{\rm NLO}(s). \quad (14)$$

The τ_2 quantity in Eq. (14) is defined by [1]

$$\tau_2 \equiv \frac{1}{4\pi}\int_0^\tau \alpha_s(\tau')d\tau' = \frac{1}{(4\pi)^2}\int_{Q_0^2}^{Q^2}\alpha_s^2(Q'^2)d\ln Q'^2, \quad (15)$$

which results from the integration of Eq. (12) with respect to τ. By substituting the expression for the differential of τ, i.e., $d\tau \equiv \frac{1}{4\pi}\alpha_s(Q'^2)d\ln Q'^2$, in the left-hand side of Eq. (15), we arrive at the right-hand side of this equation.

The required expressions in Eq. (14) are given by

$$\delta\Phi_{\rm NS}^{\rm LO}(s) \equiv \mathcal{L}[e^{-\nu}\delta P_{qq}^{\rm LO,ns}(e^{-\nu}); s],$$
$$\delta\Phi_{\rm NS}^{\rm NLO}(s) \equiv \mathcal{L}[e^{-\nu}\delta P_{qq}^{\rm NLO,NS}(e^{-\nu}); s]. \quad (16)$$

The evaluation of $\delta\Phi_{\rm NS}^{\rm NLO}(s)$ is straightforward but too lengthy to be shown here. The analytical results for the polarized splitting functions in the transformed Laplace s space at the NLO approximation are given in Appendix A.

We can find any nonsinglet solution, $\delta F_{\rm NS}(x, Q^2)$, by using the nonsinglet kernel $K_{\rm ns}(\upsilon) \equiv \mathcal{L}^{-1}[e^{\tau\delta\Phi_{\rm NS}(s)}; \upsilon]$ in the Laplace convolution relation:

$$\delta\hat{F}_{\rm NS}(\upsilon, \tau) = \int_0^\upsilon K_{\rm ns}(\upsilon - w, \tau)\delta\hat{F}_{\rm NS}^0(w)dw \quad (17)$$

and then returning to (x, Q^2) space, using the appropriate change of variable, $\upsilon \equiv \ln(1/x)$.

2. Singlet and gluon solutions

Here we wish to extend our calculations at the NLO approximation for gluon and singlet sectors of the polarized parton distributions. In this case, to decouple and solve DGLAP evolutions in Eq. (4), we need an extra Laplace transformation from τ space to U space, where s is a parameter in this new space. From now on, the $\alpha_s(\tau)/4\pi$ is replaced for brevity by $a(\tau)$. Therefore the coupled DGLAP evolution equations can be converted to

$$\begin{aligned} U\delta\mathcal{F}(s, U) - \delta f_S^0(s) &= \delta\Phi_S^{\rm LO}(s)\delta\mathcal{F}(s, U) + \delta\Phi_S^{\rm NLO}(s)\mathcal{L}[a(\tau)\delta f_S(s, \tau); U] + \delta\Theta_S^{\rm LO}(s)\delta\mathcal{G}(s, U) + \delta\Theta_S^{\rm NLO}(s)\mathcal{L}[a(\tau)\delta g(s, \tau); U], \\ U\delta\mathcal{G}(s, U) - \delta g^0(s) &= \delta\Phi_g^{\rm LO}(s)\delta\mathcal{G}(s, U) + \delta\Phi_g^{\rm NLO}(s)\mathcal{L}[a(\tau)\delta g(s, \tau); U] + \delta\Theta_g^{\rm LO}(s)\delta\mathcal{F}(s, U) + \delta\Theta_g^{\rm NLO}(s)\mathcal{L}[a(\tau)\delta f(s, \tau); U]. \end{aligned} \quad (18)$$

In writing the above expressions, we use the conventions which were introduced in Ref. [1].

The desired coupled algebraic equations for singlet and gluon distributions which are denoted in U space by $\delta\mathcal{F}(s, U)$ and $\delta\mathcal{G}(s, U)$ in Eq. (18) can be solved simultaneously, and we will arrive at

$$\delta\mathcal{F}(s,U)=\frac{(U-\delta\Phi_g)\delta f_S^0(s)}{D(U,s)}+\frac{\delta\Theta_S\delta g^0(s)}{D(U,s)},$$
$$\delta\mathcal{G}(s,U)=\frac{(U-\delta\Phi_S)\delta g^0(s)}{D(U,s)}+\frac{\delta\Theta_g\delta f_S^0(s)}{D(U,s)}. \tag{19}$$

In deriving Eq. (19), which is based on Eq. (18), we assume a simple parameterized form for $a(\tau)$ so $a(\tau)=a_0$. This will be more clarified when we consider $a(\tau)$ as a function with three unknown parameters. The denominator $D(U,s)$ in Eq. (19) has been defined in Ref. [1].

The NLO contributions of the polarized splitting functions in Laplace s space correspond to the following expressions:

$$\delta\Phi_S(s)\equiv\delta\Phi_S^{\mathrm{LO}}(s)+a_0\delta\Phi_S^{\mathrm{NLO}}(s),$$
$$\delta\Phi_g(s)\equiv\delta\Phi_g^{\mathrm{LO}}(s)+a_0\delta\Phi_g^{\mathrm{NLO}}(s),$$
$$\delta\Theta_S(s)\equiv\delta\Theta_S^{\mathrm{LO}}(s)+a_0\delta\Theta_S^{\mathrm{NLO}}(s),$$
$$\delta\Theta_g(s)\equiv\delta\Theta_g^{\mathrm{LO}}(s)+a_0\delta\Theta_g^{\mathrm{NLO}}(s). \tag{20}$$

In Eq. (20), a_0 is a parameter which can be obtained via fitting procedure as we will do in the next sections. To do more precise calculations, an excellent approximation to $a(\tau)$, accurate to a few parts in 10^4, can be given by the expression

$$a(\tau)\approx a_0+a_1e^{-b_1\tau}, \tag{21}$$

where the constants a_1 and b_1 like a_0 are found by a least-squares fit to $a(\tau)$. Therefore the Laplace transforms $\mathcal{L}[a(\tau)f(s,\tau);U]$ and $\mathcal{L}[a(\tau)g(s,\tau);U]$ needed in Eq. (18) can be written as [1]

$$\mathcal{L}[a(\tau)\delta f(s,\tau);U]=\sum_{j=0}^{1}a_j\delta\mathcal{F}(s,U+b_j),$$
$$\mathcal{L}[a(\tau)\delta g(s,\tau);U]=\sum_{j=0}^{1}a_j\delta\mathcal{G}(s,U+b_j),\quad b_0=0. \tag{22}$$

Equation (18) can be finally rewritten as

$$\begin{aligned}&[U-\delta\Phi_S(s)]\delta\mathcal{F}(s,U)-\delta\Theta_S(s)\delta\mathcal{G}(s,U)\\&\quad=\delta f^0(s)+a_1[\delta\Phi_S^{\mathrm{NLO}}(s)\delta\mathcal{F}(s,U+b_1)\\&\qquad+\delta\Theta_S^{\mathrm{NLO}}(s)\delta\mathcal{G}(s,U+b_1)],\\&-\delta\Theta_g(s)\delta\mathcal{F}(s,U)+[U-\delta\Phi_g(s)]\delta\mathcal{G}(s,U)\\&\quad=\delta g^0(s)+a_1[\delta\Theta_g^{\mathrm{NLO}}(s)\delta\mathcal{F}(s,U+b_1)\\&\qquad+\delta\Phi_g^{\mathrm{NLO}}(s)\delta\mathcal{G}(s,U+b_1)].\end{aligned} \tag{23}$$

The solutions of Eq. (23) can be obtained via an iteration process. The parameter a_0 which is inserted in expressions for the polarized splitting functions in s space [see Eq. (20)]would be quite small. To get to the solutions of Eq. (23) for $\delta\mathcal{F}$ and $\delta\mathcal{G}$, we first consider the simple solutions to Eq. (23), called $\delta\mathcal{F}_1(s,U)$ and $\delta\mathcal{G}_1(s,U)$, that result from setting $a_1=0$, i.e., the equations

$$\begin{aligned}&[U-\delta\Phi_f(s)]\delta\mathcal{F}_1(s,U)-\delta\Theta_S(s)\delta\mathcal{G}_1(U)=\delta f_S^0(s),\\&-\delta\Theta_g(s)\delta\mathcal{F}_1(U)+[U-\delta\Phi_g(s)]\delta\mathcal{G}_1(s,U)=\delta g_S^0(s),\end{aligned} \tag{24}$$

whose solutions are like Eq. (19).

We now construct an iterative solution to Eq. (23) for $\delta\mathcal{F}$ and $\delta\mathcal{G}$. To achieve the first iteration solution and in order to fulfill Eq. (22), we need to change the arguments of $\delta\mathcal{F}(s,U)$ and $\delta\mathcal{G}(s,U)$ in Eq. (24) so these functions appear as $\delta\mathcal{F}(s,U+b_1)$ and $\delta\mathcal{G}(s,U+b_1)$, respectively. Therefore the solutions of Eq. (24) for $\delta\mathcal{F}$ and $\delta\mathcal{G}$ but with the new argument as $U+b_1$ are our first approximation solutions in the iteration processes. We represent them by $\delta\mathcal{F}_1(s,U+b_1)$ and $\delta\mathcal{G}_1(s,U+b_1)$, respectively.

Now to complete the calculations and to achieve the second step of the iteration process, the parameter a_1 which before was not considered should be used. This can be done by replacement of $\delta f_S^0(s)$ and $\delta g^0(s)$ with new expressions so

$$\begin{aligned}\delta f_S^0(s)\to{}&\delta f_S^0(s)+a_1[\delta\Phi_f^{\mathrm{NLO}}(s)\delta\mathcal{F}_1(s,U+b_1)\\&+\delta\Theta_f^{\mathrm{NLO}}(s)\delta\mathcal{G}_1(s,U+b_1)],\\\delta g^0(s)\to{}&\delta g^0(s)+a_1[\delta\Theta_g^{\mathrm{NLO}}(s)\delta\mathcal{F}_1(s,U+b_1)\\&+\delta\Phi_g^{\mathrm{NLO}}(s)\delta\mathcal{G}_1(s,U+b_1)].\end{aligned} \tag{25}$$

Replacing these new expressions for $\delta f_S^0(s)$ and $\delta g^0(s)$ in Eq. (24) and solving it simultaneously will yield $\delta\mathcal{F}$ and $\delta\mathcal{G}$ at the second step of iteration, which we call $\delta\mathcal{F}_2(s,U+b_1)$ and $\delta\mathcal{G}_2(s,U+b_1)$, respectively.

Continuation of the iteration process is obvious. At the third order of iteration, we just need to replace $\delta f_S^0(s)$ and $\delta g^0(s)$ in Eq. (24) with new ones as in Eq. (25) but with the difference that in the right-hand side of this equation we should change $\delta\mathcal{F}_1(s,U+b_1)$ and $\delta\mathcal{G}_1(s,U+b_1)$ to $\delta\mathcal{F}_2(s,U+b_1)$ and $\delta\mathcal{G}_2(s,U+b_1)$. Solving Eq. (24) with these substitutions will yield $\delta\mathcal{F}$ and $\delta\mathcal{G}$, which are denoted now by $\delta\mathcal{F}_3(s,U+b_1)$ and $\delta\mathcal{G}_3(s,U+b_1)$, respectively, as the solutions at the third order of iteration.

This iteration can be continued to any required order in which we get to a sufficient convergence for the solutions. The result of iteration at higher order contains very lengthy expressions for $\delta\mathcal{F}_i$ to $\delta\mathcal{G}_i$ which make the numerical computations very hard. On the other hand, the corrections which we get up to the second order of iteration are sufficient to us to give the results in good agreement with the available experimental data and some fitting models. Therefore we here just end the calculations after two steps of iterations.

Using the inverse Laplace transform we can back from U space to τ space which will yield the following expressions for singlet and gluon distributions:

$$\delta f(s,\tau)=k_{ff}(a_1,b_1,s,\tau)\delta f_S^0(s)+k_{fg}(a_1,b_1,s,\tau)\delta g^0(s),$$
$$\delta g(s,\tau)=k_{gg}(a_1,b_1,s,\tau)\delta g^0(s)+k_{gf}(a_1,b_1,s,\tau)\delta f_S^o(s). \tag{26}$$

The analytical expressions for $k(a_1, b_1, s, \tau)$'s function up to two steps of iteration are given in Appendix B. The numerical values which we get for the unknown parameters in Eq. (22) at this order of iteration resulting from the fitting procedure are as follows: $a_0 = 0.0037$, $a_1 = 0.025$, and $b_1 = 10.7$.

After numerical Laplace inversion in Eq. (26) from s to ν space, we can write the decoupled solutions in (υ, τ) space as the convolutions defined by Eq. (9). Finally, recalling that $\nu \equiv \ln(1/x)$, the above solutions can be transformed back into the usual Bjorken-x space and virtuality Q^2, enabling us to write the NLO decoupled solutions $\delta F_s(x, Q^2)$ and $\delta G(x, Q^2)$, which require only a knowledge of $\delta F_s(x)$ and $\delta G(x)$ at Q_0^2, where evolution started. We use these analytical solutions for polarized parton distributions in the next sections to extract polarized structure functions for the proton, neutron, and deuteron.

III. POLARIZED NUCLEON STRUCTURE FUNCTION, BASED ON THE JACOBI POLYNOMIALS APPROACH

We perform here an LO and NLO fitting of the polarized parton distributions using Jacobi polynomials [12–15] to reconstruct the x-dependent quantities from their Laplace moments. The use of Jacobi polynomials has a number of benefits; specifically, it will allow us to factorize the x and Q^2 dependence in a manner that allows an efficient parametrization and evolution of the structure functions. For example, if we consider the spin structure function $xg_1(x, Q^2)$, we can expand this as

$$xg_1(x, Q^2) = x^\beta (1-x)^\alpha \sum_{n=0}^{N_{\max}} a_n(Q^2) \Theta_n^{\alpha,\beta}(x). \tag{27}$$

Here, $\Theta_n^{\alpha,\beta}(x)$ are Jacobi polynomials of order n, and $N_{\max}$ is the maximum order of our expansion. As we inferred in above, using the Jacobi polynomials has this advantage to allow us to factor out the essential part of the x dependence of the structure function into a weight function and the Q^2 dependence is contained in the Jacobi moments $a_n(Q^2)$.

To be more specific, the x dependence of the Jacobi polynomials can be written as

$$\Theta_n^{\alpha,\beta}(x) = \sum_{j=0}^{n} c_j^{(n)}(\alpha, \beta) x^j, \tag{28}$$

where the $c_j^{(n)}(\alpha, \beta)$ coefficients are combinations of Γ functions involving n, α, and β parameters. The Jacobi polynomials satisfy an orthogonality relation with weight function $x^\beta(1-x)^\alpha$ as follows:

$$\int_0^1 dx x^\beta (1-x)^\alpha \Theta_k^{\alpha,\beta}(x) \Theta_l^{\alpha,\beta}(x) = \delta_{k,l}. \tag{29}$$

Thus, given the Jacobi moments $a_n(Q^2)$, the polarized structure function $xg_1(x, Q^2)$ may be reconstructed from Eq. (27) [16,17].

We can compute the Jacobi moments $a_n(Q^2)$ by using the orthogonality relation to invert Eq. (27) to obtain

$$a_n(Q^2) = \sum_{j=0}^{n} c_j^{(n)}(\alpha, \beta) \mathcal{L}[xg_1, s = j+1]. \tag{30}$$

In Eq. (30), we have substituted Eq. (27) for $xg_1(x, Q^2)$ and employed the Laplace transformation:

$$\mathcal{L}[xg_1, s] \equiv \int_0^\infty d\upsilon e^{-s\upsilon} xg_1(x, Q^2). \tag{31}$$

On the right-hand side of Eq. (31), the x variable is taken as $e^{-\nu}$. For the final result in the left-hand side of Eq. (31), the change of variable as $\upsilon = \ln(\frac{1}{x})$ is used to back us to the usual x space. We can now relate the polarized structure function $xg_1(x, Q^2)$ with its moments [16,17] as in the following:

$$xg_1(x, Q^2) = x^\beta (1-x)^\alpha \sum_{n=0}^{N_{\max}} \Theta_n^{\alpha,\beta}(x) \times \sum_{j=0}^{n} c_j^{(n)}(\alpha, \beta) \mathcal{L}[xg_1, s = j+1]. \tag{32}$$

Given Eq. (32) for $xg_1(x, Q^2)$, we choose the set $\{N_{\max}, \alpha, \beta\}$ to achieve optimal convergence of this series throughout the kinematic region constrained by the data. In practice, we find $N_{\max} = 9$, $\alpha = 3.0$, and $\beta = 0.5$ to be sufficient. We are then able to express xg_1 in terms of nine unknown parameters, for instance, at an input scale of $Q_0^2 = 4$ GeV^2. We now examine the fits to the spin structure functions to extract the PPDFs from the available data.

IV. QCD ANALYSIS OF PPDFS AND THE PARAMETRIZATION

A. Parametrization

We consider a proton comprised of massless partons with helicity distributions $q_\pm(x, Q^2)$ which carry momentum fraction x with a characteristic scale Q. The difference $\delta q(x, Q^2) = q_+(x, Q^2) - q_-(x, Q^2)$ measures how much the parton of flavor q "remembers" of the parent proton polarization. We will parameterize these PPDFs at initial scale $Q_0^2 = 4$ GeV^2 using the following form:

$$x\delta q(x, Q_0^2) = \mathcal{N}_q \eta_q x^{a_q} (1-x)^{b_q} (1 + c_q x), \tag{33}$$

where the polarized PDFs are determined by parameters $\{\eta_q, a_q, b_q, c_q\}$ and the generic label $q = \{u_v, d_v, \bar{q}, g\}$ denotes the partonic flavors up-valence, down-valence, sea, and gluon, respectively. The normalization constants $\mathcal{N}_q$,

$$\frac{1}{\mathcal{N}_q} = \left(1 + c_q \frac{a_q}{a_q + b_q + 1}\right) B(a_q, b_q + 1), \tag{34}$$

are chosen such that η_i are the first moments of $\delta q_i(x, Q_0^2)$, where $B(a, b)$ is the Euler beta function.

The total up and down PPDFs are a sum of the valence plus sea distributions: $\delta u = \delta u_v + \delta\bar{q}$ and $\delta d = \delta d_v + \delta\bar{q}$. We will assume an $SU(3)$ flavor symmetry such that $\delta\bar{q} \equiv \delta\bar{u} = \delta\bar{d} = \delta s = \delta\bar{s}$, while we could allow for an $SU(3)$ symmetry violation term by introducing κ such that $\delta s = \delta\bar{s} = \kappa\delta\bar{q}$, as the strange PPDF is poorly constrained. The results would be insensitive to the specific choice of κ.

As seen from Eq. (33), each of the four polarized parton densities $q = \{u_v, d_v, \bar{q}, g\}$ contains four parameters $\{\eta_q, a_q, b_q, c_q\}$, which gives a total of 16 parameters which should be determined. We now demonstrate that we can eliminate some of these parameters while maintaining sufficient flexibility to obtain a good fit.

1. First moments of δu_v and δd_v

The parameters η_{u_v} and η_{d_v} are the first moments of the δu_v and δd_v polarized valence quark densities; these quantities can be related to F and D as measured in neutron and hyperon β decays according to the following relations [18]:

$$a_3 = \int_0^1 dx\delta q_3 = \eta_{u_v} - \eta_{d_v} = F + D, \tag{35}$$

$$a_8 = \int_0^1 dx\delta q_8 = \eta_{u_v} + \eta_{d_v} = 3F - D, \tag{36}$$

where a_3 and a_8 are the nonsinglet combinations of the first moments of the polarized parton densities corresponding to

$$\delta q_3 = (\delta u + \delta\bar{u}) - (\delta d + \delta\bar{d}), \tag{37}$$

$$\delta q_8 = (\delta u + \delta\bar{u}) + (\delta d + \delta\bar{d}) - 2(\delta s + \delta\bar{s}). \tag{38}$$

A reanalysis of F and D with updated β-decay constants will yield $F = 0.464 \pm 0.008$ and $D = 0.806 \pm 0.008$ [18]. With these values we find

$$\eta_{u_v} = +0.928 \pm 0.014, \tag{39}$$

$$\eta_{d_v} = -0.342 \pm 0.018. \tag{40}$$

The errors of parameters in Eqs. (39) and (40) are the systematical ones, and we fix the numerical values of these parameters in our fit. Therefore we make use of η_{u_v} and η_{d_v} to reduce the number of parameters by two.

2. Gluon and sea quarks

We find that the factor $(1 + c_q x)$ in Eq. (33) provides flexibility to obtain a good description of the data, particularly for the valence distributions u_v and d_v. Thus we will make use of the c_q coefficients for the up-valence and down-valence distributions; in contrast, we are able to set the values for $c_{\bar{q}}$ and c_g to zero ($c_{\bar{q}} = c_g = 0$) while maintaining a good fit and eliminating two free parameters. For the c_{u_v} and c_{d_v} parameters, we find the fit improves if we use nonzero values, but as these are relatively flat directions in χ space we shall fix the values as detailed in Table I.

Separately, we find that the b parameters control the large-x behavior of the PPDFs; thus, the sea quark and

TABLE I. Final parameter values and their statistical errors in the $\overline{\text{MS}}$ scheme at the input scale $Q_0^2 = 4$ GeV^2, in the LO and NLO approximations.

		LO			
δu_v	η_{u_v}	0.928 (fixed)	$\delta\bar{q}$	$\eta_{\bar{q}}$	-0.0661 ± 0.0315
	a_{u_v}	0.197 ± 0.0035		$a_{\bar{q}}$	0.258 ± 0.04763
	b_{u_v}	2.325 ± 0.0481		$b_{\bar{q}}$	8.3 (fixed)
	c_{u_v}	20.45 (fixed)		$c_{\bar{q}}$	0
δd_v	η_{d_v}	-0.342 (fixed)	δg	η_g	3.393 ± 3.072
	a_{d_v}	0.234 ± 0.0169		a_g	0.837 ± 1.67
	b_{d_v}	3.129 ± 0.138		b_g	2.797 (fixed)
	c_{d_v}	30.0 (fixed)		c_g	0
		$\Lambda = 0.289 \pm 0.017$ GeV			
		χ^2/D.O.F. $= 305.21/370 = 0.824$			
		NLO			
δu_v	η_{u_v}	0.928 (fixed)	$\delta\bar{q}$	$\eta_{\bar{q}}$	-0.0599 ± 0.0022
	a_{u_v}	0.339 ± 0.022		$a_{\bar{q}}$	0.814 ± 0.0356
	b_{u_v}	2.434 ± 0.032		$b_{\bar{q}}$	3.124 (fixed)
	c_{u_v}	28.9 (fixed)		$c_{\bar{q}}$	0
	η_{d_v}	-0.342 (fixed)	δg	η_g	2.623 ± 0.551
	a_{d_v}	0.199 ± 0.0084		a_g	5.895 (fixed)
	b_{d_v}	2.373 ± 0.0769		b_g	9.34 (fixed)
	c_{d_v}	26.57 (fixed)		c_g	0
		$\Lambda = 0.2011 \pm 0.0441$ GeV			
		χ^2/D.O.F. $= 300.205/370 = 0.811$			

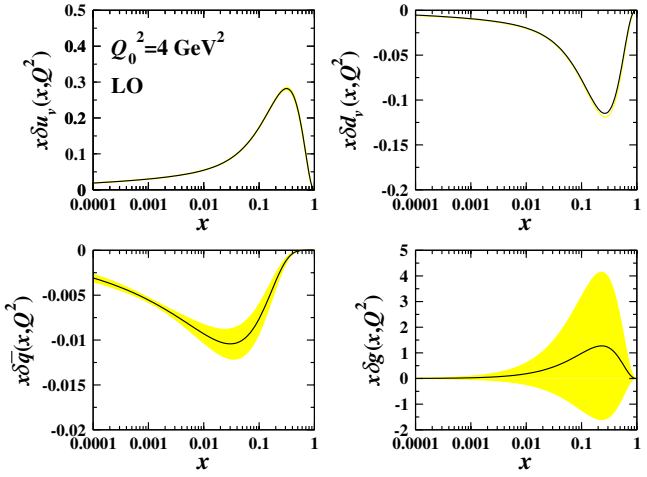

FIG. 1 (color online). The polarized quark densities in the LO approximation as a function of x at initial energy scale $Q_0^2 = 4$ GeV^2, resulting from our fit. Yellow (light gray) regions indicate the error bands.

gluon distributions have large uncertainties in this region, as they are dominated by the valence. To provide some guidance, we observe that, for the polarized parton densities in the large-x region, a ratio of $b_{\bar{q}}/b_g \sim 1.6$ provides a good fit. Therefore we impose this ratio on the polarized $b_{\bar{q}}$ and b_g parameters to further reduce the free parameters. Additionally, we are able to extract reasonable constraints on the $a_{\bar{q}}$ and a_g parameters; this is a benefit of the Jacobi polynomials.

Having fixed η_{u_v}, η_{d_v}, $c_{\bar{q}}$, and c_g parameters and the ratio $b_{\bar{q}}/b_g$ in preliminary minimization, we then set the $b_{\bar{q}}$, b_g, c_{u_v}, and c_{d_v} parameters as indicated in Table I; this gives us a total of nine unknown parameters, in addition to $\alpha_s(Q_0^2)$.

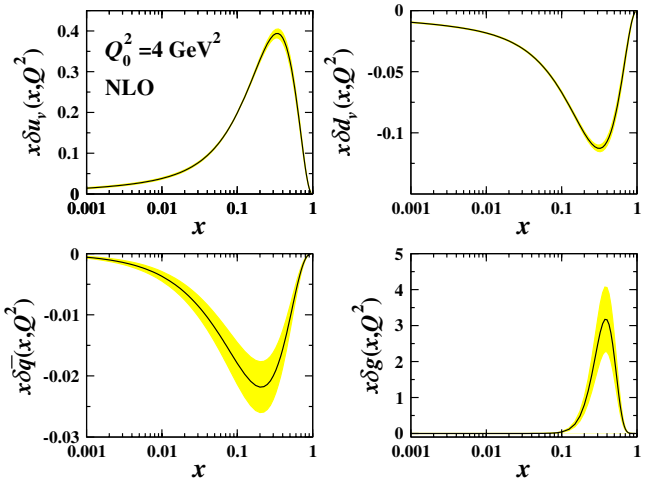

FIG. 2 (color online). The polarized quark densities in the NLO approximation as a function of x at initial energy scale $Q_0^2 = 4$ GeV^2, resulting from our fit. Yellow (light gray) regions indicate the error bands.

Having equipped to required inputs, we depict in Figs. 1 and 2 our predictions for PPDFs at $Q_0^2 = 4$ GeV^2 which we choose as the initial energy scale in the fit.

B. DGLAP evolution

In the Jacobi polynomial approach, the DGLAP evolution equations can be solved in the Laplace space. The Laplace transformation of the parton densities δq are defined analogous to that of Eq. (31) as follows:

$$\begin{aligned}\mathcal{L}[\delta q(x=e^{-v},Q_0^2),s] &\equiv \delta q(s,Q_0^2)\\ &= \int_0^\infty e^{-sv}\delta q(x=e^{-v},Q_0^2)dv\\ &= \mathcal{N}_q\eta_q\left(1+c_q\frac{s+a_q}{s+a_q+b_q+1}\right)B(s+a_q,b_q+1),\end{aligned} \tag{41}$$

where $q = \{u_v, d_v, \bar{q}, g\}$ and B is the Euler beta function.

In the Laplace space, the LO contribution to the polarized proton and neutron structure function, $xg_1(s, Q^2)$, can be represented in terms of the polarized parton densities by

$$\mathcal{L}[xg_1^p, s] = \frac{1}{2}\sum_q e_q^2 \times [\delta q(s,Q^2) + \delta\bar{q}(s,Q^2)], \tag{42}$$

$$\mathcal{L}[xg_1^n, s] = \mathcal{L}[xg_1^p, s] - \frac{1}{6}(\mathcal{L}[u_v, s] - \mathcal{L}[d_v, s]). \tag{43}$$

At the NLO approximation, the polarized structure function $xg_1^p(s, Q^2)$ and $xg_1^n(s, Q^2)$ in s space can be written by

$$\begin{aligned}\mathcal{L}[xg_1^p, s] = \sum_q e_q^2\Big[\frac{1}{2}\Big(1+\frac{\tau}{4\pi}\delta c_q(s)\Big)\times(\delta q(s,Q^2)\\ + \delta\bar{q}(s,Q^2)) + \frac{2}{3}\Big(\frac{\tau}{4\pi}\delta c_g(s)\times\delta g(s,Q^2)\Big)\Big],\end{aligned} \tag{44}$$

$$\begin{aligned}\mathcal{L}[xg_1^n, s] = \mathcal{L}[xg_1^p, s] - \frac{1}{6}(\mathcal{L}[u_v, s]\\ - \mathcal{L}[d_v, s])\Big(1+\frac{\tau}{4\pi}\times\delta c_q(s)\Big).\end{aligned} \tag{45}$$

Here, the sum runs over u, d, s quark flavors, and the polarized quark, antiquark, and gluon distributions are represented by δq, $\delta\bar{q}$, and δg, respectively. The analytical expressions for Wilson coefficients $\delta c_q(s)$ and $\delta c_g(s)$ in Laplace transform s space are given in Appendix A.

C. The g_2 structure function

Now, by having the g_1 structure function, one can calculate the g_2 structure function in the LO and NLO approximation via the Wandzura-Wilczek [19,20] expression as in the following:

$$g_2(x,Q^2) = -g_1^p(x,Q^2) + \int_x^1 \frac{dy}{y}g_1^p(y,Q^2). \tag{46}$$

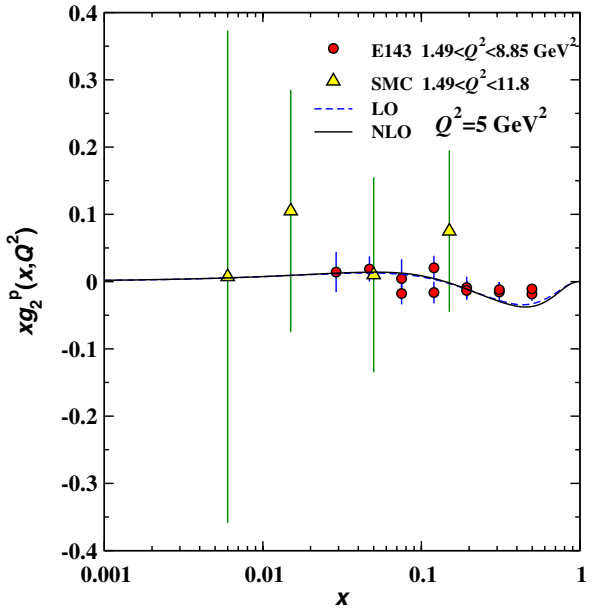

FIG. 3 (color online). The polarized structure function xg_2 at $Q^2 = 5$ GeV^2 as a function of x in LO and NLO approximations. A comparison with the available experimental data [21,22] has also been done.

Figure 3 shows our prediction for xg_2 in comparison with the available experimental data from the Spin Muon Collaboration (SMC) [21] and E143 [22] data groups which are in very good agreement with them.

V. QCD FIT OF $xg_1(x, Q^2)$ DATA

In our analysis, we investigate the QCD evolution of the massless parton densities at the LO and NLO approximation, using a number of active flavors, $N_f = 3$ in the fixed-flavor number scheme. These assumptions make our fitting procedure efficient numerically. For the polarized proton structure functions, we use the European Muon Collaboration (EMC) [23], HERMES [24,25], SMC [21], E143 [22], E155 [26], and COMPASS [27] data. For the neutron one, the E142 [28], HERMES [24,25], and E154 [29,30] data have been used, and for the deuteron, we use the data from SMC [21], E143 [22], E155 [31], and HERMES [24] experimental groups. In Table II, we list briefly the related information of the used data.

We minimize the global χ^2 as follows [32–34]:

$$\chi^2_{\text{global}} = \sum_n w_n \chi^2_n, \tag{47}$$

where the sum n runs over the different experiments, w_n is a weight factor for the data of the nth experiment, and χ^2_n is given by

$$\chi^2_n = \left(\frac{1 - \mathcal{N}_n}{\Delta \mathcal{N}_n}\right)^2 + \sum_i \left(\frac{\mathcal{N}_n g^{\text{exp}}_{1,i} - g^{\text{theor}}_{1,i}}{\mathcal{N}_n \Delta g^{\text{exp}}_{1,i}}\right)^2. \tag{48}$$

Here, $g^{\text{exp}}_{1,i}$, $\Delta g^{\text{exp}}_{1,i}$, and $g^{\text{theor}}_{1,i}$ denote the experimental measurement, the experimental uncertainty (statistical and systematic combined in quadrature), and theoretical

TABLE II. Published data points with the measured x and Q^2 ranges, including the number of data points (with a cut of $Q^2 \geq 1.0$ GeV^2) and the fitted normalization shifts $\mathcal{N}_i$.

Experiment	x range	Q^2 range [GeV^2]	# of data points	$\mathcal{N}_i$
E143 (p)	0.031–0.749	1.27–9.52	28	0.995 69
HERMES (p)	0.028–0.66	1.01–7.36	39	1.0010
SMC (p)	0.005–0.480	1.30–58.0	12	0.999 62
EMC (p)	0.015–0.466	3.50–29.5	10	1.0021
E155	0.015–0.750	1.22–34.72	24	1.015 78
HERMES06 (p)	0.026–0.731	1.12–14.29	51	0.997 29
COMPASS10 (p)	0.005–0.568	1.10–62.10	15	0.988 17
Proton			179	
E143 (d)	0.031–0.749	1.27–9.52	28	1.001 19
E155 (d)	0.015–0.750	1.22–34.79	24	1.001 37
SMC (d)	0.005–0.479	1.30–54.80	12	0.999 99
HERMES06 (d)	0.026–0.731	1.12–14.29	51	1.0019
Deuteron			115	
E142 (n)	0.035–0.466	1.10–5.50	8	0.999 89
HERMES (n)	0.033–0.464	1.22–5.25	9	0.999 89
E154 (n)	0.017–0.564	1.20–15.00	17	1.000 37
HERMES06 (n)	0.026–0.731	1.12–14.29	51	1.002 08
Neutron			85	
Total			379	

value for the ith data point, respectively. $\Delta\mathcal{N}_n$ is the experimental normalization uncertainty, and $\mathcal{N}_n$ is an overall normalization factor for the data of the nth experiment. We allow for a relative normalization shift $\mathcal{N}_n$ between different data sets within uncertainties $\Delta\mathcal{N}_n$ quoted by the experiments.

We minimize the above χ^2 value with the nine unknown parameters. The values of these parameters are summarized in Table I. We find $\chi^2/\text{d.o.f.} = 305.21/370 = 0.824$ for LO approximation and $\chi^2/\text{d.o.f.} = 300.21/370 = 0.811$ for the NLO approximation, which is less than the LO one as we are expecting and yields an acceptable fit to the experimental data.

VI. THE ANALYSIS OF THE ERROR CALCULATIONS

The evolved polarized parton densities and structure functions are attributive functions of the input parameters. Let $q(x, Q^2; p_i|_{i=1}^k)$ be the evolved distribution at Q^2 depending on the parameters $p_i|_{i=1}^k$. Then its correlated error as given by Gaussian error propagation is [35]

$$\Delta\delta q(x, Q^2) = \left\{\sum_{i=1}^{k}\left(\frac{\partial\delta q}{\partial p_i}\right)^2 C(p_i, p_i) + \sum_{i\neq j=1}^{k}\left(\frac{\partial\delta q}{\partial p_i}\frac{\partial\delta q}{\partial p_j}\right)C(p_i, p_j)\right\}^{\frac{1}{2}}, \quad (49)$$

where $C(p_i, p_j)$ are the elements of the covariance matrix obtained in the QCD fit procedure at the scale Q_0^2. The covariance matrix does not change when the evolution is done in Mellin or Laplace space. That means it can be used at any scale of Q^2. The gradients $\partial\delta q/\partial p_i$ at this scale can be calculated analytically. Its value at Q^2 is calculated by evolution, and the gradients evolved in desired space are then transformed back to x space and are used according to Eq. (49). Here we give an example of the gradient for the polarized valence distributions $q = u_v, d_v$ in Laplace space, based on the final variable parameter a_q:

$$\frac{\partial\mathcal{L}[\delta q](s)}{\partial a_q} = \left(B(s+a_q, 1+b_q)\left(-\frac{(1+b_q)d_q(s+a_q+b_q+1+(s+a_q)d_q)}{(1+a_q+b_q)^2(s+a_q+b_q+1)} - (\psi(a_q) - \psi(1+a_q+b_q))\right.\right.$$
$$\times\left(1+\frac{a_q d_q}{1+a_q+b_q}\right)\left(1+\frac{(s+a_q)d_q}{s+a_q+b_q+1}\right) + (\psi(s+a_q) - \psi(s+1+a_q+b_q))\left(1+\frac{a_q d_q}{1+a_q+b_q}\right)$$
$$\left.\left.\times\left(1+\frac{(s+a_q)d_q}{s+1+a_q+b_q}\right) + \frac{(1+b_q)d_q(1+b_q+a_q(1+d_q))}{(1+a_q+b_q)(s+1+a_q+b_q)^2}\right)\eta_q\right)\Big/\left(B(a_q, 1+b_q)\left(1+\frac{a_q d_q}{1+a_q+b_q}\right)^2\right). \quad (50)$$

This equation helps us to obtain the required gradients to follow the error calculations for the polarized structure functions g_1^p, g_1^n, and g_1^d.

A. Neighborhood of global minimum via Hessian method

Here we just present the essential points of the Hessian method. The full procedure is provided in Refs. [36–38].

As we mentioned in the first part of Sec. V, we can find a set of the appropriate parameters which minimize the global χ^2 function and denote this PPDF set by S_0. Let us present these parameters by $p_1^0 \ldots p_n^0$ as we did in Sec. VI. By moving the parameters away from their obtained values, χ^2_{global} increases by the amount of $\Delta\chi^2_{\text{global}}$:

$$\Delta\chi^2_{\text{global}} = \chi^2_{\text{global}} - \chi^2_0 = \sum_{i,j=1}^{d} H_{ij}(p_i - p_i^0)(p_j - p_j^0), \quad (51)$$

where the Hessian matrix H_{ij} is defined by

$$H_{ij} = \frac{1}{2}\frac{\partial^2\chi^2_{\text{global}}}{\partial p_i \partial p_j}\bigg|_{\text{min}}, \quad (52)$$

and we note that in Eq. (49) $C \equiv H^{-1}$. Now it is convenient to work in terms of the eigenvalues and eigenvectors of covariance matrix

$$\sum_{j=1}^{n} C_{ij}v_{jk} = \lambda_k v_{ik}, \quad (53)$$

where C_{ij} is the ijth component of covariance matrix and λ_k and v_{ik} are the kth eigenvalue and ith component of the kth eigenvector, respectively. Also the displacement of parameter p_i from its minimum p_i^0 can be expressed in terms of rescaled eigenvectors $e_{ik} = \sqrt{\lambda_k}v_{ik}$:

$$p_i - p_i^0 = \sum_{k=1}^{n} e_{ik}z_k. \quad (54)$$

Replacing Eq. (54) in Eq. (51) and considering the orthogonality of v_k, we obtain

$$\Delta\chi^2_{\text{global}} = \sum_{k=1}^{n} z_k^n. \quad (55)$$

Now the relevant neighborhood of χ^2_{global} is the interior of the hypersphere with radius T:

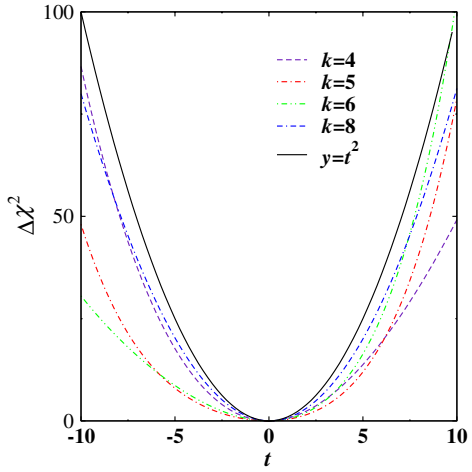

FIG. 4 (color online). $\Delta\chi^2$ as a function of t for some random sample eigenvectors in the LO approximations. The solid line is the ideal case, $\Delta\chi^2 = t^2$.

$$\sum_{k=1}^{n} z_k^2 \leq T^2, \tag{56}$$

and the neighborhood parameters are given by

$$p_i(s_k^{\pm}) = p_i^0 \pm t e_{ik}, \tag{57}$$

where s_k is the kth set of PPDFs and t is adapted to make the desired $T = (\Delta\chi^2_{\text{global}})^{\frac{1}{2}}$ and $t = T$ in the quadratic approximation. In Sec. V, we indicated the dependence of $\Delta\chi^2_{\text{global}}$ along some random samples of eigenvector directions to test the quadratic approximation of Eq. (51).

In the preliminary QCD fit process we let all input parameters vary and investigate the global behavior of $\Delta\chi^2$. We observe global $\Delta\chi^2$ increase consumedly in some points, and a big amount of redundance in parameters happens. This redundancy results in disorder of quadratic behavior of global $\Delta\chi^2$. In order for the Hessian method to work well, we need to fix some parameters at their best obtained values so that the Hessian matrix depends on the number of parameters which are independent sufficiently for the quadratic behavior of global $\Delta\chi^2$. To complete the calculations, we need to detail constraints in parameter space along some random samples of eigenvector directions and eigenvalues. The curves for some values of λ_k are very close to the ideal quadratic curve $\Delta\chi^2 = t^2$ as can be seen in Figs. 4 and 5 at LO and NLO approximations. Therefore we see some departure of the ideal quadratic curve, which indicates that the quadratic approximation is almost adequate, though imperfect.

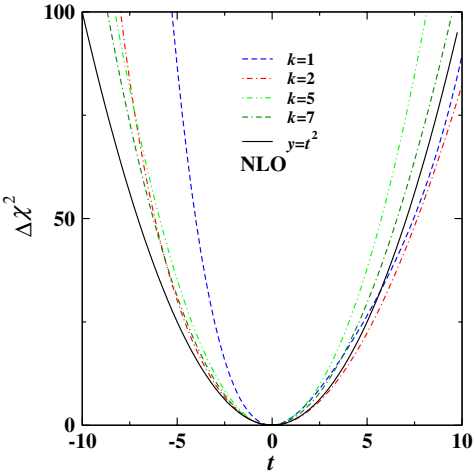

FIG. 5 (color online). $\Delta\chi^2$ as a function of t defined for some random sample eigenvectors at the NLO approximations. The solid line is the ideal case, $\Delta\chi^2 = t^2$.

VII. RESULTS AND DISCUSSION

In this section we present the results that have been obtained for the PPDFs, using the Laplace transformation technique to solve analytically the DGLAP evolution equations. We depict in Fig. 6 the polarized proton structure function at the LO approximation in which comparison with the available experimental data and some fitting parametrization models has also been done. In Fig. 7, we plot at LO and NLO approximations the proton, neutron, and deuteron structure functions at different energy scales and compare them with available experimental data [22]. To avoid having the figures with crowded plots, the comparison with some fitting parametrization models has been discarded in this figure and the following ones. In Fig. 8, we compare our results for the nonsinglet spin structure function $[g_1^{\text{NS}} = \frac{1}{6}(\delta u_v(x)) - \delta d_v(x))]$ with those from SMC, E143, and HERMES Collaborations [21,22,24,39]. We use from the SMC data group and depict in Fig. 9 the xg_1^p structure function at $Q^2 = 10\ \text{GeV}^2$ in the LO and

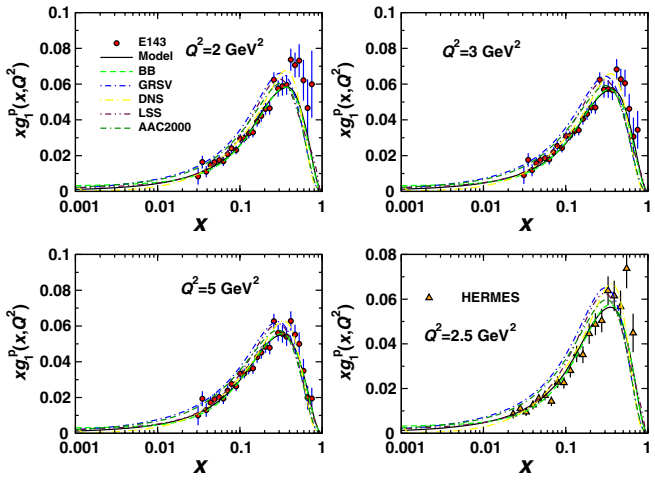

FIG. 6 (color online). Proton spin structure function, resulting from our model (solid curve) at LO approximation and its comparison with some fitting parameterizations [35,43–46] and SMC [21], E143 [22], and HERMES [25] experimental data groups.

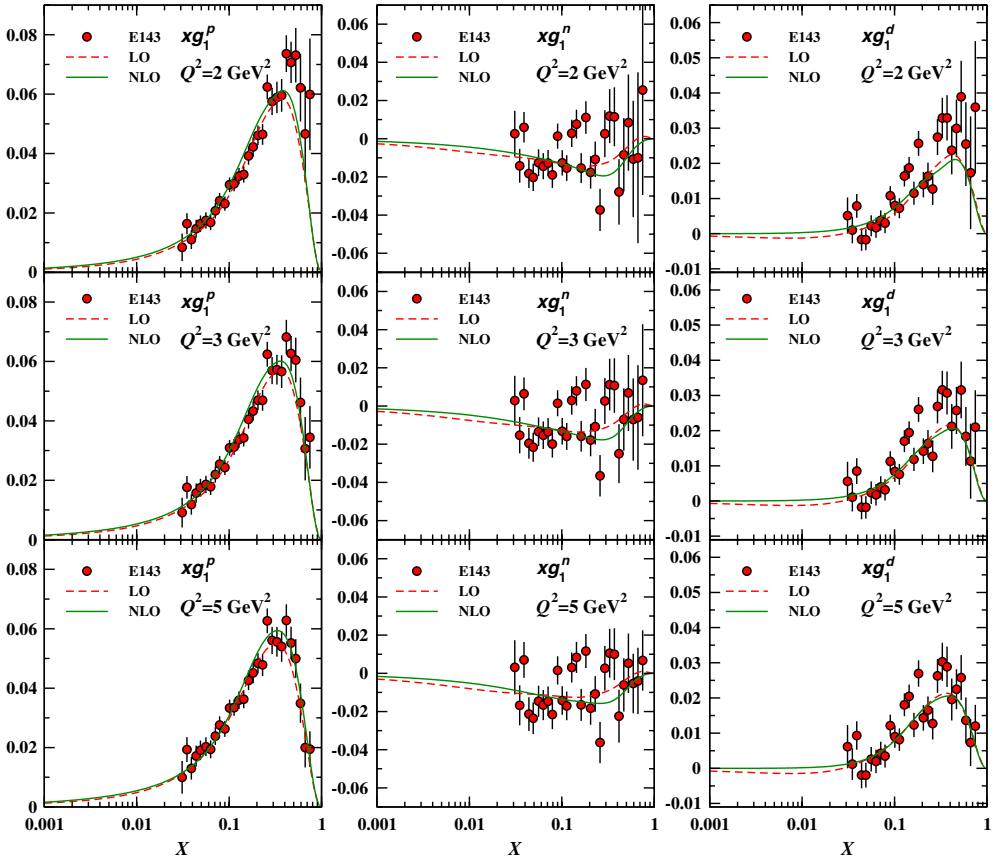

FIG. 7 (color online). Proton, neutron, and deuteron spin structure functions at LO and NLO approximations with E143 experimental data [22].

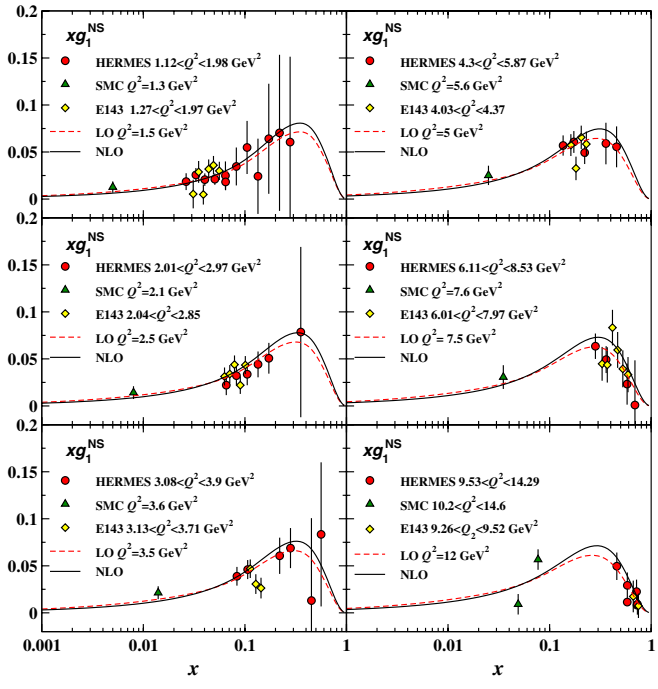

FIG. 8 (color online). Nonsinglet spin structure function at LO and NLO approximations. A comparison with the available experimental data SMC [21,39], E143 [22], and HERMES [24] has also been done.

NLO approximations. The comparison with the experimental data indicates an improvement of the NLO result with respect to the LO one. In Fig. 10, the same story is repeated and comparison with the E154 data group is done [30].

The first moment for PPDFs can be calculated in Laplace space. Therefore we can find the contribution of

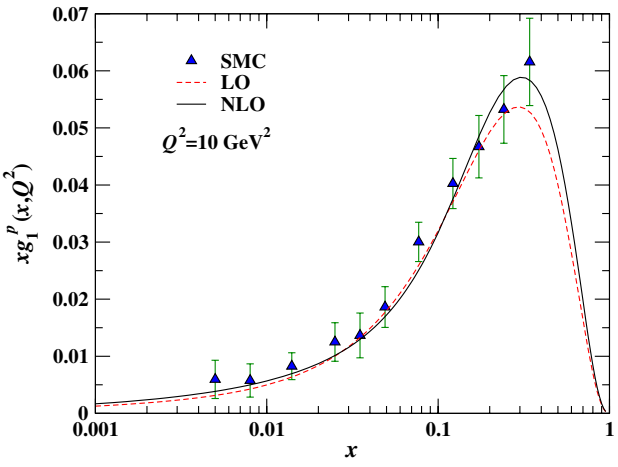

FIG. 9 (color online). Proton spin structure function at the LO and NLO approximations at $Q^2 = 10$ GeV^2 and its comparison with SMC experimental data [22].

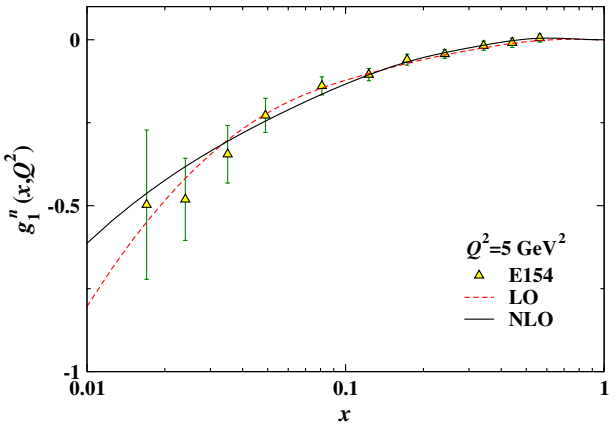

FIG. 10 (color online). Neutron spin structure function at the LO and NLO approximations at $Q^2 = 5$ GeV^2 and its comparison with the available experimental data [30].

each parton to the spin of the proton. In the LO approximation, the first moments for valence and sea distributions are constant, and only the first moment for the gluon changes by Q^2. For PPDFs at $Q^2 = 4$ GeV^2 we get

$$\Delta u_v = 0.928, \qquad \Delta d_v = -0.342, \qquad \Delta \bar{q} = -0.066\,1596, \qquad \Delta g = 3.393\,28. \tag{58}$$

For the gluon distribution at $Q^2 = 100$ GeV^2 we get $\Delta g = 4.626\,63$, which indicates that the first moment of the gluon polarization has been changed dominantly with respect to its previous value, as we expect. At the NLO approximation these first moments are not constant and will change by Q^2. The results are tabulated in Table III. The behaviors of changing the first moments with respect to Q^2 are as we expect and confirm the validity of our calculations.

In our QCD fitting analysis, the universal transmuted cutoff parameter Λ is a free parameter. So we can achieve the numerical value of the Λ parameter in the $\overline{\text{MS}}$ scheme, as indicated in Table I. We can then estimate the renormalized coupling constant $\alpha_s(Q^2)$ at different values of Q^2. At $Q_0^2 = 4$ GeV^2 and in the NLO approximation we get the numerical value $\alpha_s(Q_0^2) = 0.2194 \pm 0.0178$, and at the scale of Z boson mass we get $\alpha(M_z^2) = 0.1177 \pm 0.0042$, which are in good agreement with what was reported in Refs. [40,41].

TABLE III. The first moment of the valence, sea, and gluon polarization in the NLO approximation at different values of Q^2, resulting from our analysis.

Q^2	1 GeV^2	10 GeV^2	20 GeV^2	200 GeV^2
Δu_v	0.928 167	0.927 917	0.927 834	0.927 602
Δd_v	−0.342 061	−0.341 969	−0.341 939	−0.341 853
$\Delta \bar{q}$	−0.060 193 8	−0.079 779 8	−0.099 576 9	−0.118 883
Δg	2.256 38	2.835 73	2.991 13	3.469 68

By integrating Eq. (32) we can calculate the Γ_1^p at $Q^2 = 10$ GeV^2 and obtain

$$\Gamma_1^p = 0.128\,191, \quad \Gamma_1^n = -0.0580497, \quad \Gamma_1^d = 0.0320196$$

at LO approximation, and at the NLO approximation we get

$$\Gamma_1^p = 0.128\,988, \quad \Gamma_1^n = -0.0670665, \quad \Gamma_1^d = 0.0282673,$$

which are in good agreement with what has been reported in Refs. [17,42].

VIII. CONCLUSION

In this paper, we used the Laplace transformation technique to extract the PPDFs inside the nucleon. Our main gradient of this paper was to apply the method of Block *et al.* in Refs. [1–3] to the polarized case. Following this method, using the Laplace transformation, we indicated that this method works well in which we were able to extract the polarized parton distribution functions for the nonsinglet, singlet, and gluon densities.

In continuation of our calculation, we obtained the polarized proton and neutron structure functions. At first we focused on the valence quark polarization inside the nucleon and calculated the nonsinglet sector of the spin structure function. We then extended our calculations to the polarized gluon and singlet sectors. We finally extracted the polarized nucleon and deuteron structure functions at different values of Q^2 in LO and NLO approximations of QCD analysis.

The calculation in the LO approximation could be done by just one Laplace transformation from $x = e^{\nu}$ space to s space. At the NLO approximation, we needed additionally the second Laplace transformation from τ space to what was called U space. The solutions for the singlet and gluon distributions at NLO approximation could be done by an iteration which we followed in this paper up to the second order.

The advantage of the analytical solutions for the PPDFs in Laplace transformed s space is that it enables us to achieve strictly analytical solutions for the parton densities in terms of the Bjorken-x variable. We do not have this ability when we use the Mellin moments, where in that case the calculations can be followed just numerically. Using this technique has its own benefits from the point of its transparency to make us able to dominate over the details of calculations more straightforwardly.

As an auxiliary technique, we employed the Jacobi polynomial approach to achieve the polarized nucleon structure function in the (x, Q^2) plane while we used the moments of PPDFs in s-(Laplace) space. We discussed also how the parameterizations are obtained by emphasis on computing the χ^2_{global}, covariant, and Hessian matrices.

By accessing the analytical solutions for the polarized parton distributions which lead us to the polarized nucleon structure functions, it is straightforward to extend the calculations to obtain the structure functions for nuclei which

can be considered a new research task in the future. Using other orthogonal hypergeometrical functions rather than the Jacobi polynomials in the fit, say, for instance, Hermit polynomials, might make easier the fit and would be an interesting subject to follow in our further research activity.

ACKNOWLEDGMENTS

F. T.-S. and S. A. T. acknowledge the institute for research in fundamental sciences (IPM) for their hospitality while this research was performed. S. A. T. is thankful to Yazd Branch, Islamic Azad University for supporting him financially for this project.

APPENDIX A

We present here the results for the different splitting and Wilson coefficient functions, denoted by C_q and C_g at the NLO approximation, in the Laplace transformed, s space.

$$
\begin{aligned}
\Phi_{\mathrm{NS}\pm}^{\mathrm{NLO}} = {} & C_f^2\Big(\frac{3}{8}-\frac{\pi^2}{2}-\frac{1}{(s+1)^3}-\frac{5}{s+1}-\frac{1}{(s+2)^3}+\frac{2}{(s+2)^2}+\frac{5}{s+2}+\frac{1}{(s+1)^2}+2(\gamma_E+\psi(s+2)\\
& -(s+1)\psi'(s+2))\frac{1}{(s+2)^2}2(\gamma_E+\psi(s+3)-(s+2)\psi'(s+3))\\
& -4\Big((\gamma_E+\psi(s+1))\psi'(s+1)-\frac{1}{2}\psi''(s+1)\Big)+6\zeta(3)+3\psi'(s+1)\Big)\\
& +C_fC_a\Big(\frac{17}{24}+\frac{11\pi^2}{18}-\frac{1}{(s+1)^3}+\frac{5}{6(s+1)^2}+\frac{53}{18(s+1)}+\frac{\pi^2}{6(s+1)}-\frac{1}{(s+2)^3}\\
& +\frac{5}{6(s+2)^2}-\frac{187}{18(s+2)}+\frac{\pi^2}{6(s+2)}-3\zeta(3)-\frac{11}{3}\psi'(s+1)-\psi''(s+1)\Big)+C_fT_f\Big(-\frac{1}{6}-\frac{2\pi^2}{9}-\frac{2}{3(s+1)^2}\\
& -\frac{2}{9(s+1)}-\frac{2}{3(s+2)^2}+\frac{22}{9(s+2)}+\frac{4}{3}\psi'(s+1)\Big)\mp\Big(C_f^2-\frac{1}{2}C_aC_f\Big)\Big(\frac{2}{(s+1)^3}-\frac{2}{(s+1)^2}+\frac{4}{s+1}-\frac{\pi^2}{3(s+1)}\\
& -\frac{2}{(s+2)^3}-\frac{2}{(s+2)^2}+\frac{0.04}{s+2}+\frac{\pi^2}{3(s+2)}+\frac{4}{(s+3)^3}-\frac{9.972}{s+4}+\frac{2\pi^2}{3(s+4)}+\frac{4}{(s+5)^3}-\frac{10.952}{s+5}-\frac{2\pi^2}{3(s+5)}\\
& -\frac{4}{(s+6)^3}+\frac{10.092}{s+6}+\frac{2\pi^2}{3(s+6)}-\frac{12.616}{s+7}+\frac{2.44}{s+8}-\frac{3.328}{s+9}\frac{0.856}{s+10}-\frac{0.208}{s+11}+\frac{4.4}{s+12}+\frac{1}{(s+1)^3}\\
& \times\Big(-8+(s+1)\ln(16)+2(s+1)\psi\Big(1+\frac{s}{2}\Big)-2(1+s)\psi\Big(\frac{s+1}{2}\Big)-(s+1)^2\Big(\psi'\Big(1+\frac{s}{2}\Big)-\psi'\Big(\frac{s+1}{2}\Big)\Big)\Big)\\
& -\frac{1}{(s+2)^3}\Big(\frac{16}{(s+1)^2}+\frac{12s}{(s+1)^2}+(s+2)\ln(16)-2(s+2)\psi\Big(1+\frac{s}{2}\Big)+2(s+2)\psi\Big(\frac{s+1}{2}\Big)\\
& +(s+2)^2\Big(\psi'\Big(1+\frac{s}{2}\Big)-\psi'\Big(\frac{s+1}{2}\Big)\Big)\Big)-\frac{1}{(s+3)^3}2\Big(\frac{164+284s+188s^2+60s^3+8s^4}{(s+1)^2(s+2)^2}\\
& -4(s+3)\ln(2)-2(s+3)\psi\Big(1+\frac{s}{2}\Big)+2(s+3)\psi\Big(\frac{s+1}{2}\Big)+(s+3)^2\Big(\psi'\Big(1+\frac{s}{2}\Big)-\psi'\Big(\frac{s+1}{2}\Big)\Big)\Big)\\
& -\frac{2}{(s+4)^3}\Big(\frac{2176+4392s+3504s^2 1408s^3+288s^4+24s^5}{(s+1)^2(s+2)^2(s+3)^2}+4(s+4)\ln(2)\\
& -2(s+4)\Big(\psi\Big(1+\frac{s}{2}\Big)-\psi\Big(\frac{s+1}{2}\Big)\Big)+(s+4)^2\Big(\psi'\Big(1+\frac{s}{2}\Big)-\psi'\Big(\frac{s+1}{2}\Big)\Big)\Big)\\
& -\frac{1}{(s+5)^3}2\Big(\frac{57328+146144s+162160s^2+103728s^3+42144s^4+11160s^5+1880s^6+184s^7+8s^8}{(s+1)^2(s+2)^2(s+3)^2(s+4)^2}\\
& -4(s+5)\ln(2)-2(s+5)\Big(\psi\Big(1+\frac{s}{2}\Big)+\psi\Big(\frac{s+1}{2}\Big)\Big)+(s+5)^2\Big(\psi\Big(1+\frac{s}{2}\Big)-\psi\Big(\frac{s+1}{2}\Big)\Big)\Big)\\
& -\frac{1}{(s+6)^2}2\Big(\ln(16)-2\psi\Big(4+\frac{s}{2}\Big)+2\psi\Big(\frac{s+7}{2}\Big)+(s+6)\psi'\Big(4+\frac{s}{2}\Big)-(s+6)\psi'\Big(\frac{s+7}{2}\Big)\Big)\Big),
\end{aligned}
\tag{A1}
$$

$$
\delta\Phi_{qq}^{\mathrm{NLO}}(s) = 2C_fT_f\Big(-\frac{2}{(s+1)^3}+\frac{1}{(s+1)^2}+\frac{1}{s+1}-\frac{2}{(s+2)^3}-\frac{3}{(s+2)^2}-\frac{1}{s+2}\Big),
\tag{A2}
$$

$$
\begin{aligned}
2f\delta\Theta_f^{\mathrm{NLO}} = C_a T_f\Big(&-\frac{4}{(s+1)^3}-\frac{2}{(s+1)^2}+\frac{24}{s+1}-\frac{2\pi^2}{3(s+1)}+\frac{8}{(s+2)^3}-\frac{16}{(s+2)^2}-\frac{22}{s+2}+\frac{4\pi^2}{3(s+2)}-\frac{0.656}{s+3}\\
&-\frac{3.964}{s+4}+\frac{10.228}{s+5}+\frac{2.744}{s+6}-\frac{6.392}{s+7}+\frac{4.4}{s+8}+\frac{8}{s+1}(\gamma_E+\psi(s+2))-\frac{8}{s+2}(\gamma_E+\psi(s+3))+\frac{1}{(s+1)^3}\Big)\\
&\times\Big(-8+(s+1)\ln(16)+2(s+1)\psi\Big(1+\frac{s}{2}\Big)-2(s+1)\psi\Big(\frac{s+1}{2}\Big)(s+1)^2\psi'\Big(1+\frac{s}{2}\Big)+(s+1)^2\psi'\Big(\frac{s+1}{2}\Big)\Big)\\
&-\frac{2}{(s+2)^2}\Big(\frac{16}{(s+1)^2}+\frac{12s}{(s+1)^2}+(s+2)\ln(16)-2(s+2)\psi\Big(1+\frac{s}{2}\Big)+2(s+2)\psi\Big(\frac{s+1}{2}\Big)\\
&+(s+2)^2\psi'\Big(1+\frac{s}{2}\Big)-(s+2)^2\psi'\Big(\frac{s+1}{2}\Big)\Big)+\frac{2}{6(s+1)}(\pi^2+6(\gamma_E+\psi(s+2))^2-6\psi'(s+2))\\
&-\frac{4}{6s+12}(\pi^2+6(\gamma_E+\psi(s+3))^2-6\psi'(s+3))+C_f T_f\Big(-\frac{2}{(s+1)^3}+\frac{9}{(s+1)^2}-\frac{22}{s+1}+\frac{2\pi^2}{3(s+1)}\\
&+\frac{4}{(s+2)^3}+\frac{27}{s+2}-\frac{4\pi^2}{3(s+2)}-\frac{8}{s+1}(\gamma_E+\psi(s+2))+\frac{8}{s+2}(\gamma_E+\psi(s+3))\\
&-\frac{2}{6s+6}(\pi^2+6(\gamma_E+\psi(s+2))^2-6\psi'(s+2)+\frac{4}{(s+1)^2}(\gamma_E+\psi(s+2))-(s+1)\psi'(s+2)\\
&+\frac{4}{6s+12}(\pi^2+6(\gamma_E+\psi(s+3))^2-6\psi'(s+3))-\frac{8}{(s+2)^2}((\gamma_E+\psi(s+3))-(s+2)\psi'(s+3))\Big),
\end{aligned}
\tag{A3}
$$

$$
\begin{aligned}
\delta\Theta_g^{\mathrm{NLO}} = C_f T_f\Big(&-\frac{16}{9(s+1)}-\frac{4}{9(s+2)}+\frac{8}{3(s+1)}(\gamma_E+\psi(s+2))-\frac{4}{3(s+2)}(\gamma_E+\psi(s+3))\Big)C_f^2\Big(\frac{2}{(s+1)^3}+\frac{2}{(s+1)^2}-\frac{9}{2(s+1)}\\
&-\frac{1}{(s+2)^3}-\frac{1}{2(s+2)^2}+\frac{2}{(s+1)}(\gamma_E+\psi(s+2))\frac{1}{s+2}(\gamma_E+\psi(s+3))-\frac{1}{6s+6}(\pi^2+6(\gamma_E+\psi(s+2))^2-6\psi'(s+2))\Big)\\
&+C_a C_f\Big(\frac{5}{(s+1)^3}-\frac{4}{(s+1)^2}+\frac{41}{9(s+1)}-\frac{\pi^2}{6(s+1)}-\frac{5}{2(s+2)^3}+\frac{13}{(s+2)^2}+\frac{35}{9(s+2)}+\frac{\pi^2}{12(s+2)}+\frac{0.328}{s+3}+\frac{2.474}{s+4}\\
&-\frac{1.157}{s+5}-\frac{1.129}{s+6}+\frac{1.624}{s+7}-\frac{0.55}{s+8}-\frac{10}{3(s+1)}(\gamma_E+\psi(s+2))-\frac{1}{3(s+2)}(\gamma_E+\psi(s+3))-\frac{1}{2(s+1)^3}\\
&\times\Big(-8(s+1)\ln(16)2(s+1)\psi\Big(1+\frac{s}{2}\Big)-2(s+1)\psi\Big(\frac{s+1}{2}\Big)-(s+1)^2\Big(\psi'\Big(1+\frac{s}{2}\Big)+\psi'\Big(\frac{s+1}{2}\Big)\Big)\Big)\\
&+\frac{1}{4(s+2)^3}\Big(\frac{16}{(s+1)^2}+\frac{12s}{(s+1)^2}+(2+s)\ln(16)-2(s+2)\psi\Big(1+\frac{s}{2}\Big)+\frac{2}{6s+6}(\pi^2+6(\gamma_E+\psi(s+2))^2-6\psi'(s+2))\\
&-\frac{4}{(s+1)^2}((\gamma_E+\psi(s+2))-(s+1)\psi'(s+2)-\frac{1}{6s+12}(\pi^2+6(\gamma_E+\psi(s+3))^2-6\psi'(s+3))\\
&+\frac{2}{(s+2)^2}(\gamma_E+\psi(s+3))^2-(s+2)\psi'(s+3))\Big),
\end{aligned}
\tag{A4}
$$

$$
\begin{aligned}
\delta\Phi_g^{\mathrm{NLO}} = &-C_f T_f\Big(1+\frac{4}{(s+1)^3}-\frac{10}{(s+1)^2}+\frac{10}{s+1}+\frac{4}{(s+2)^3}+\frac{2}{(s+2)^2}-\frac{10}{s+2}\Big)-C_a T_f\Big(\frac{4}{3}-\frac{4}{3(s+1)^2}+\frac{56}{9(s+1)}\\
&-\frac{4}{3(s+2)^2}-\frac{76}{9(s+2)}\Big)+C_a^2\Big(12.5456754+\frac{4}{(s+1)^3}+\frac{134}{9(s+1)}-\frac{2\pi^2}{3(s+1)}-\frac{8}{(s+2)^3}-\frac{268}{9(s+2)}\\
&+\frac{4\pi^2}{3(s+2)}-\frac{67}{9}(\gamma_E+\psi(s+1))+\frac{1}{3}\pi^2(\gamma_E+\psi(s+1)-\frac{1}{9}(-67+3\pi^2)(\gamma_E+\psi(s+1))\\
&-\frac{8}{(s+1)^2}(\gamma_E+\psi(s+2)-(s+1)\psi'(s+2))+\frac{16}{(s+2)^2}(\gamma_E+\psi(s+3)-(s+1)\psi'(s+3))\\
&-4\Big((\gamma_E+\psi(s+1))\psi'(s+1)-\frac{1}{2}\psi''(s+1)\Big)-\psi''(s+1)\Big),
\end{aligned}
\tag{A5}
$$

$$C_q = -\frac{4}{3}\left(\frac{9}{2}+\frac{\pi^2}{3}\right)+\frac{8}{3(s+2)}+\frac{4}{3(s+2)}+\frac{4(\gamma_E+\psi(s+2))}{3(s+1)}+\frac{4(\gamma_E+\psi(s+3))}{3(s+2)}+\frac{4}{3}\psi'(s+1)+\frac{4}{3}\psi'(s+3), \tag{A6}$$

$$C_g = \frac{1}{2}\left(\frac{2}{s+1}-\frac{2}{s+2}+\frac{\gamma_E+\psi(s+1)}{s+1}-\frac{2(\gamma_E+\psi(s+2))}{s+2}\right). \tag{A7}$$

APPENDIX B

We bring in below the coefficients of singlet and gluon distributions of Eq. (26), $k(a_1, b_1, s, \tau)$'s, in the Laplace transformed, s space.

$$\begin{aligned}
k_{ff} = {} & \frac{1}{2R(s)b_1(R^2(s)-b_1^2)}e^{\frac{1}{2}\tau(\delta\Phi_f+\delta\Phi_g-R(s)-2b_1)}\Big(2a_1e^{\frac{R(s)\tau}{2}}b_1^2\Big(2\sinh\Big(\frac{\tau R(s)}{2}\Big)\delta\Theta_f\delta\Theta_g-(-1+e^{\tau b_1})\delta\Phi_f \\
& \times\Big(R(s)\cosh\Big(\frac{\tau R(s)}{2}\Big)+\sinh\Big(\frac{\tau R(s)}{2}\Big)(\delta\Phi_f-\delta\Phi_g)\Big)\Big)4a_1e^{\frac{1}{2}\tau(R(s)+b_1)}\sinh\Big(\frac{\tau b_1}{2}\Big)\Big(R^2(s)\sinh\Big(\frac{\tau R(s)}{2}\Big) \\
& \times(\delta\Theta_f\delta\Theta_g+\delta\Phi_f(\delta\Phi_f-\delta\Phi_g))+R(s)\cosh\Big(\frac{\tau R(s)}{2}\Big)(\delta\Phi_f(\delta\Phi_f-\delta\Phi_g)^2+\delta\Theta_f\delta\Theta_g(3\delta\Phi_f-\delta\Phi_g)) \\
& -e^{\tau b_1}b_1^3(R(s)-\delta\Phi_f+e^{R(s)\tau}(R(s)+\delta\Phi_f-\delta\Phi_g)+\delta\Phi_g)+b_1\Big(e^{\tau b_1}(\delta\Phi_f-\delta\Phi_g)^2(R(s)-\delta\Phi_f \\
& +e^{R(s)\tau}(R(s)\delta\Phi_f-\delta\Phi_g)+\delta\Theta_f\delta\Theta_g\Big(a_1(R(s)-\delta\Phi_f-\delta\Phi_g+e^{R(s)\tau}(R(s)+\delta\Phi_f+\delta\Phi_g))+2e^{\frac{1}{2}\tau(R(s)+2b_1)} \\
& \times\Big((4-a_1)R(s)\cosh\Big(\frac{\tau R(s)}{2}\Big)+\sinh\Big(\frac{\tau R(s)}{2}\Big)((4+a_1)\delta\Phi_f-(4-a_1)\delta\Phi_g)\Big)\Big)\Big)\Big)\Big),
\end{aligned} \tag{B1}$$

$$\begin{aligned}
k_{fg} = {} & \frac{1}{2R(s)b_1(R^2(s)-b_1^2)}e^{\frac{1}{2}\tau(\delta\Phi_f+\delta\Phi_g-R(s)-2b_1)}\delta\Theta_f\Big(-2e^{\tau b_1}(-1+e^{\tau b_1})b_1^3+4a_1e^{\frac{1}{2}\tau(R(s)+2b_1)}\sinh\Big(\frac{\tau b_1}{2}\Big) \\
& \times\Big(R(s)\cosh\Big(\frac{\tau R(s)}{2}\Big)(2\delta\Theta_f\delta\Theta_g+\delta\Phi_f(\delta\Phi_f-\delta\Phi_g))+R^2(s)\sinh\Big(\frac{\tau R(s)}{2}\Big)\delta\Phi_f\Big)-4a_1e^{\frac{1}{2}\tau(r+b_1)}b_1^2\Big(\sinh\Big(\frac{\tau b_1}{2}\Big) \\
& \times\Big(R(s)\cosh\Big(\frac{\tau R(s)}{2}\Big)+\delta\Phi_f\sinh\Big(\frac{\tau R(s)}{2}\Big)\Big)-\delta\Phi_g\cosh\Big(\frac{\tau b_1}{2}\Big)\sinh\Big(\frac{\tau R(s)}{2}\Big)\Big) \\
& +b_1\Big(2(-1+e^{\tau R(s)})(a_1+(4+a_1)e^{\tau b_1})\delta\Theta_f\delta\Theta_g+a_1\delta\Phi_g(R(s)+\delta\Phi_f-\delta\Phi_g+e^{\tau R(s)}(R(s)-\delta\Phi_f-\delta\Phi_g)) \\
& +2e^{\frac{1}{2}\tau(R(s)+2b_1)}-a_1R(s)\cosh\Big(\frac{\tau R(s)}{2}\Big)\delta\Phi_g+\sinh\Big(\frac{\tau R(s)}{2}\Big)(-\delta\Phi_f+\delta\Phi_g)(-2\delta\Phi_f+(2+a_1)\delta\Phi_g)\Big)\Big),
\end{aligned} \tag{B2}$$

$$\begin{aligned}
k_{gf} = {} & \frac{1}{R(s)b_1(-R^2(s)+b_1^2)}2e^{\frac{1}{2}\tau(\delta\Phi_f+\delta\Phi_g-b_1)}\delta\Theta_g\Big(e^{\frac{\tau b_1}{2}}\sinh\Big(\frac{\tau R(s)}{2}\Big)b_1(b_1^2-4\delta\Theta_f\delta\Theta_g-(\delta\Phi_f-\delta\Phi_g)^2) \\
& +a_1\Big(-\cosh\Big(\frac{\tau b_1}{2}\Big)\sinh\Big(\frac{\tau R(s)}{2}\Big)b_1(2\delta\Theta_f\delta\Theta_g+\delta\Phi_f(b_1+\delta\Phi_f-\delta\Phi_g))+\sinh\Big(\frac{\tau b_1}{2}\Big)\Big(\sinh\Big(\frac{\tau R(s)}{2}\Big) \\
& \times(b_1^2-R^2(s))\delta\Theta_g+R(s)\cosh\Big(\frac{\tau R(s)}{2}\Big)(-2\delta\Theta_f\delta\Theta_g+(b_1+\delta\Phi_f-\delta\Phi_g)(b_1+\delta\Phi_g))\Big)\Big)\Big),
\end{aligned} \tag{B3}$$

$$k_{gg} = \frac{1}{R(s)b_1(-R^2(s)+b_1^2)} e^{\frac{1}{2}\tau(\delta\Phi_f+\delta\Phi_g-2b_1)}\Big((-1+e^{\tau b_1})a_1\Big(R(s)\cosh\Big(\frac{\tau R(s)}{2}\Big)(-\delta\Theta_f\delta\Theta_g(\delta\Phi_f-3\delta\Phi_g)$$
$$+(-b_1^2+(\delta\Phi_f-\delta\Phi_g)^2)\delta\Phi_g)+\sinh\Big(\frac{\tau R(s)}{2}\Big)(R^2(s)\delta\Theta_f\delta\Theta_g+(R^2(s)-b_1^2)\delta\Phi_g(-\delta\Phi_f+\delta\Phi_g))\Big)$$
$$+b_1\Big(\sinh\Big(\frac{\tau R(s)}{2}\Big)\delta\Phi_f^3+a_1\delta\Theta_f\delta\Theta_g\Big(R(s)\cosh\Big(\frac{\tau R(s)}{2}\Big)+\sinh\Big(\frac{\tau R(s)}{2}\Big)(2b_1+\delta\Phi_f+\delta\Phi_g)\Big)\Big)$$
$$+e^{\tau b_1}b_1\Big(R(s)\cosh\Big(\frac{\tau R(s)}{2}\Big)(-b_1^2+(4-a_1)\delta\Theta_f\delta\Theta_g+(\delta\Phi_f-\delta\Phi_g)^2)+\sinh\Big(\frac{\tau R(s)}{2}\Big)(b_1^2(\delta\Phi_f-\delta\Phi_g)$$
$$+\delta\Theta_f\delta\Theta_g((-4+a_1)\delta\Phi_f+(4+a_1)\delta\Phi_g)+\delta\Phi_g(3\delta\Phi_f^2-3\delta\Phi_f\delta\Phi_g+\delta\Phi_g^2))\Big)\Big). \quad \text{(B4)}$$

[1] M. M. Block, L. Durand, P. Ha, and D. W. McKay, Eur. Phys. J. C **69**, 425 (2010).
[2] M. M. Block, L. Durand, P. Ha, and D. W. McKay, Phys. Rev. D **84**, 094010 (2011).
[3] M. M. Block, L. Durand, P. Ha, and D. W. McKay, Phys. Rev. D **83**, 054009 (2011).
[4] M. M. Block, Eur. Phys. J. C **65**, 1 (2010).
[5] M. M. Block, Eur. Phys. J. C **68**, 683 (2010).
[6] M. M. Block, L. Durand, P. Ha, and D. W. McKay, arXiv:1004.1440.
[7] F. Taghavi-Shahri, A. Mirjalili, and M. M. Yazdanpanah, Eur. Phys. J. C **71**, 1590 (2011).
[8] V. N. Gribov and L. N. Lipatov, Yad. Fiz. **15**, 781 (1972) [Sov. J. Nucl. Phys. **15**, 438 (1972)].
[9] G. Altarelli and G. Parisi, Nucl. Phys. **B126**, 298 (1977).
[10] Y. L. Dokshitzer, Zh. Eksp. Teor. Fiz. **73**, 1216 (1977) [Sov. Phys. JETP **46**, 641 (1977)].
[11] W. Furmanski and R. Petronzio, Z. Phys. C **11**, 293 (1982).
[12] A. L. Kataev, A. V. Kotikov, G. Parente, and A. V. Sidorov, Phys. Lett. B **417**, 374 (1998).
[13] A. L. Kataev, G. Parente, and A. V. Sidorov, arXiv:hep-ph/9809500.
[14] A. L. Kataev, G. Parente, and A. V. Sidorov, Nucl. Phys. **B573**, 405 (2000).
[15] A. L. Kataev, G. Parente, and A. V. Sidorov, Phys. Part. Nucl. **34**, 20 (2003); Nucl. Phys. B, Proc. Suppl. **116**, 105 (2003).
[16] S. Atashbar Tehrani and A. N. Khorramian, J. High Energy Phys. 07 (2007) 048.
[17] A. N. Khorramian, S. Atashbar Tehrani, F. Olness, S. Taheri Monfared, and F. Arbabifar, Nucl. Phys. B, Proc. Suppl. **207–208**, 65 (2010).
[18] C. Amsler *et al.* (Particle Data Group), Phys. Lett. B **667**, 1 (2008).
[19] S. Wandzura and F. Wilczek, Phys. Lett. **72B**, 195 (1977).
[20] A. Piccione and G. Ridolfi, Nucl. Phys. **B513**, 301 (1998).
[21] B. Adeva *et al.* (Spin Muon Collaboration), Phys. Rev. D **58**, 112001 (1998).
[22] K. Abe *et al.* (E143 Collaboration), Phys. Rev. D **58**, 112003 (1998).
[23] J. Ashman *et al.* (European Muon Collaboration), Phys. Lett. B **206**, 364 (1988); Nucl. Phys. **B328**, 1 (1989).
[24] A. Airapetian *et al.* (HERMES Collaboration), Phys. Rev. D **75**, 012007 (2007).
[25] K. Ackerstaff *et al.* (HERMES Collaboration), Phys. Lett. B **404**, 383 (1997); A. Airapetian *et al.* (HERMES Collaboration), Phys. Lett. B **442**, 484 (1998).
[26] P. L. Anthony *et al.* (E155 Collaboration), Phys. Lett. B **493**, 19 (2000).
[27] M. G. Alekseev *et al.* (COMPASS Collaboration), Phys. Lett. B **690**, 466 (2010); V. Y. Alexakhin *et al.* (COMPASS Collaboration), Phys. Lett. B **647**, 8 (2007).
[28] P. L. Anthony *et al.* (E142 Collaboration), Phys. Rev. D **54**, 6620 (1996).
[29] K. Abe *et al.* (E154 Collaboration), Phys. Lett. B **405**, 180 (1997).
[30] K. Abe *et al.* (E154 Collaboration), Phys. Rev. Lett. **79**, 26 (1997).
[31] P. L. Anthony *et al.* (E155 Collaboration), Phys. Lett. B **463**, 339 (1999).
[32] D. Stump, J. Pumplin, R. Brock, D. Casey, J. Huston, J. Kalk, H. Lai, and W. Tung, Phys. Rev. D **65**, 014012 (2001).
[33] A. N. Khorramian and S. A. Tehrani, Phys. Rev. D **78**, 074019 (2008).
[34] A. N. Khorramian, H. Khanpour, and S. A. Tehrani, Phys. Rev. D **81**, 014013 (2010).
[35] J. Blumlein and H. Bottcher, Nucl. Phys. **B636**, 225 (2002).
[36] A. D. Martin, R. G. Roberts, W. J. Stirling, and R. S. Thorne, Eur. Phys. J. C **28**, 455 (2003).
[37] A. D. Martin, W. J. Stirling, R. S. Thorne, and G. Watt, Eur. Phys. J. C **63**, 189 (2009).
[38] J. Pumplin, D. Stump, R. Brock, D. Casey, J. Huston, J. Kalk, H. L. Lai, and W. K. Tung, Phys. Rev. D **65**, 014013 (2001).

[39] B. Adeva *et al.* (Spin Muon Collaboration), Phys. Rev. D **60**, 072004 (1999); **62**, 079902(E) (2000).
[40] J. Santiago and F. J. Yndurain, Nucl. Phys. **B611**, 447 (2001).
[41] A. L. Kataev, Proc. Sci., ACAT2007 (2007) 072.
[42] T. Gehrmann and W. J. Stirling, Z. Phys. C **65**, 461 (1995).
[43] E. Leader, A. V. Sidorov, and D. B. Stamenov, Phys. Rev. D **75**, 074027 (2007).
[44] Y. Goto *et al.* (Asymmetry Analysis Collaboration), Phys. Rev. D **62**, 034017 (2000).
[45] M. Gluck, E. Reya, M. Stratmann, and W. Vogelsang, Phys. Rev. D **63**, 094005 (2001).
[46] D. de Florian, G. A. Navarro, and R. Sassot, Phys. Rev. D **71**, 094018 (2005).